Line shapes for electron-hole plasmas in semiconductors. I. The heavy-hole to spin-orbit split-band transitions in electron-hole droplets in Ge

C. H. Aldrich and R. N. Silver

Testing and Theoretical Divisions, Los Alamos Scientific Laboratory, Los Alamos, New Mexico 87545

(Received 30 April 1979)

We report details of a new theory for the luminescence and absorption line shapes of electron-hole plasmas in semiconductors. The theory includes the physical processes which lead to the creation of single-plasmon or particle-hole pairs. It is the extension to line-shape problems of the random-phase approximation which has been successful for the thermodynamic properties of electron-hole liquids. Extensive calculations are presented and compared to experiments on the cross section for absorption due to heavy-hole to spin-orbit split-band transitions in electron-hole droplets in Ge. Good agreement with the observed broad line shape is obtained when details of the valence-band structure of Ge are included. In an appendix, we present an analysis of the dielectric function in the spherical model for the $\vec{k}\cdot\vec{p}$ valence-band Hamiltonian of diamond and zinc-blende semiconductors for finite spin-orbit splitting.

I. INTRODUCTION

Our understanding of electron-hole condensates in highly excited semiconductors has been largely acquired by the study of their optical transitions.[1] The simplest theory for the line shapes assumes that electrons and holes act as free particles inside conduction and valence bands renormalized by the many-body interactions. This "free-particle theory" has successfully explained the line shape for electron-hole-droplet (EHD) luminescence in indirect semiconductors apart from a weak low-energy tail.[2] In indirect transitions, phonons take up the momentum difference between initial and final states. However, in direct transitions, where momentum must be conserved, the free-particle theory is less successful. The gain spectra of highly excited direct semiconductors are better fit by an assumption of no momentum conservation.[3] Large-broadening parameters are required to fit transitions between heavy-hole and light-hole bands responsible for the plasmon width in EHD in Ge.[4] The most striking example of the failure of the free-particle theory has been the absorption due to transitions between heavy-hole and spin-orbit-split bands in EHD in Ge.[5] The observed absorption is much broader than the free-particle prediction as shown in Fig. 1.

Theories for the deviations from free-particle theory have in common that they take into account physical processes which leave the electron-hole plasma in an excited state.[6,7] Scattering of electrons and holes with the creation of elementary excitations in the plasma will cause apparent deviations from the momentum conservation required for direct transitions. However, the theories differ in the methods of calculating these effects and in their agreement with experiment.

In this paper, we discuss details of a new theory for the line shapes of electron-hole plasmas. We take the heavy-hole to spin-orbit-split band

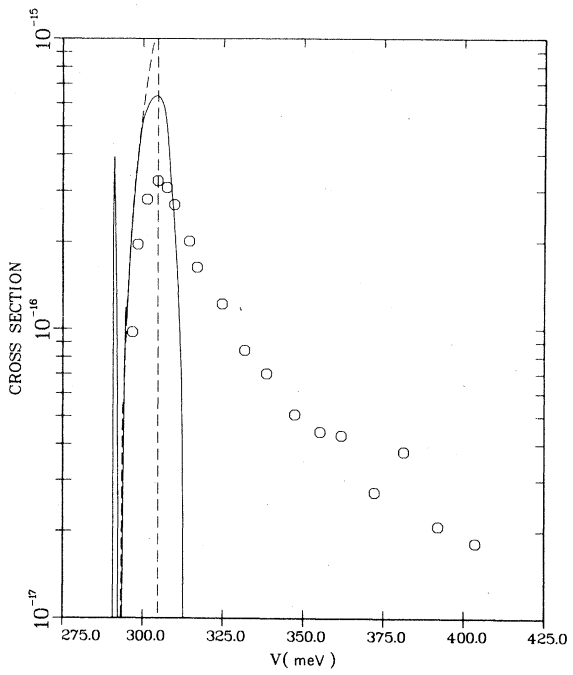

FIG. 1. Comparison between the free-particle theory and experiment (Pokrovsky and Svistunova, Ref. 5) for intervalence band transitions in electron-hole droplets in Ge. The dashed curve uses the spherical model for the valence-band structure. The solid curve keeps the spherical-model matrix elements but uses the full anisotropy of the effective masses. The lower-energy peak is due to light-hole to spin-orbit-split band transitions. The higher-energy peak is due to heavy-hole to spin-orbit split-band transitions.

transitions in electron-hole droplets as a quantitative test of the theory. We show that the line shape may be understood within the random-phase approximation which has previously been successful for thermodynamic properties.[8] Agreement with experiment requires taking into account both the creation of elementary excitations and details of the valence-band structure of Ge.

This paper is a detailed account of work which has previously appeared in preliminary form elsewhere.[9,10] The arguments presented herein are largely intuitive. A later paper will discuss the derivation of our results from the standpoint of formal kinetic and transport theory.[11]

The organization of this paper is as follows. Section II reviews previous theories for the line shapes of electron-hole plasmas. Section III discusses the qualitative physics of our approach to line shapes taking the case of heavy-hole to spin-orbit-split band transitions as both motivation and illustration. Section IV contains our detailed calculations for these transitions. Section V contains concluding remarks and a discussion of the implications of our theory for other transitions. Appendix A contains details of the dielectric function for zinc-blende semiconductors for finite spin-orbit splitting in the spherical approximation. Appendix B contains details of the multiple-scattering arguments in Sec. III.

II. REVIEW OF PREVIOUS THEORIES FOR LINE SHAPES

A. Comparison of the free-particle theory and experiment

The spherical approximation to the valence-band structure of diamond and zinc-blende semiconductors is illustrated schematically in Fig. 2 and developed in detail in Appendix A. In electron hole droplets, the hole bands are filled up to a Fermi level marked ϵ_F. In this paper, we are concerned with transitions between the two degenerate hole bands and the spin-orbit split band. Since photons carry negligible momentum, these transitions must be direct in the absence of scattering processes, i.e., they must be vertical in Fig. 2. For an initial hole in the heavy-hole band, the highest momentum a final hole in the spin-orbit split band can attain is the Fermi momentum. Thus, the free-hole theory predicts a sharp cutoff in the absorption at a frequency marked ν_c. There is also a sharp threshold at the spin-orbit splitting marked $\nu_{\rm th}$. The light-hole band which contains only ~5% of holes contributes a very narrow absorption below $\nu_{\rm th}$ which also has a sharp cutoff. The existence of a cutoff frequency ν_c and a threshold frequency $\nu_{\rm th}$ is retained when the spherical approximation is replaced with the fully anisotropic band structure.

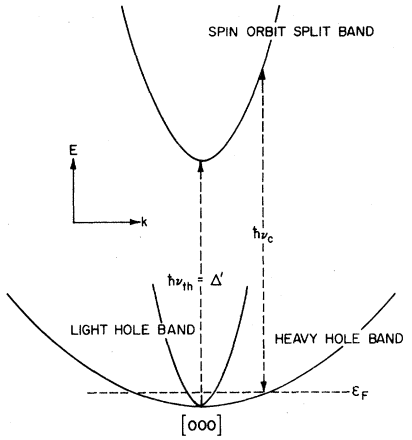

FIG. 2. Schematic valence-band structure of Ge in the spherical model. The spin-orbit splitting Δ' is renormalized by the many-body interactions in electron-hole droplets. The hole states in these bands are occupied up to a Fermi level ϵ_F. Three is a sharp threshold $\nu_{\rm th}$ for hole to spin-orbit-split band transitions. In the free-particle theory transitions between bands must be vertical (conserve k). There is a sharp cutoff at ν_c corresponding to the momentum of a final particle in the spin-orbit-split band equal to the Fermi momentum in the heavy-hole band. The existence of a $\nu_{\rm th}$ and ν_c in the free-particle theory is not altered by the extension to anisotropic bands.

Calculations in the free hole theory using the matrix elements derived in Appendix A are shown in Fig. 1. The dashed curve is the result for the spherical approximation. The solid curve retains the spherical model matrix elements but uses the fully anisotropic effective masses. The dots are the measurements of Pokrovsky and Svistunova[5] normalized close to the cross section of 3×10^{-17} cm^2 at 3.3 μm measured by Worlock *et al.*[12] It is clear that the free-hole theory is inadequate.

We believe that the physical phenomena responsible for the deviation from the free particle theory are the same in our example and in several other transitions. For the purpose of later discussion, we therefore rewrite the free-particle theory in the general terms of a transition rate between two bands labeled 1 and 2. The free-particle formula is then for direct transitions

$$I_1^2(\hbar\nu) = \int d^3k\,[1-f(\epsilon_k^1)]f(\epsilon_k^2)|\,M_{\vec{k}}\,|^2 \times \delta(\hbar\nu - E_g' - \epsilon_{\vec{k}}^1 + \epsilon_{\vec{k}}^2), \quad (1)$$

where the f are Fermi functions, E_g' is a renormalized gap energy, $M_{\vec{k}}$ is a matrix element which may be $\vec{k}$ dependent, and the $\epsilon_{\vec{k}}^i$ are the energies in band i. In our example, band 1 is

the spin-orbit-split band, 2 is the heavy-hole band, E_g' the renormalized spin-orbit splitting, and $M_{\vec{k}}$ is $O(|\vec{k}|^1)$.

B. Landsberg theory

Landsberg[6] observes that an electron above the Fermi surface or a hole below it can decay by the creation of an elementary excitation in the electron hole plasma. The initial and final states in a transition should therefore be broadened by their widths such as can be calculated within the random-phase approximation (RPA). Formula (1) is modified to

$$I_1^2(\hbar\nu) = \int d^3k[1-f(\epsilon_{\vec{k}}^1)]f(\epsilon_{\vec{k}}^2)|M_{\vec{k}}|^2 \frac{1}{\pi} \frac{\Gamma^1(\epsilon_{\vec{k}}^1)+\Gamma^2(\epsilon_{\vec{k}}^2)}{(\hbar\nu - E_g - \epsilon_{\vec{k}}^1 + \epsilon_{\vec{k}}^2)^2 + [\Gamma^1(\epsilon_{\vec{k}}^1)+\Gamma^2(\epsilon_{\vec{k}}^2)]^2}, \tag{2}$$

where $\Gamma^1(\epsilon_{\vec{k}}^1)$ is the RPA width in band 1. Several authors have claimed success for this approach for the gain spectra of direct-gap semiconductors[13] and of analogous formulas for EHD luminescence in indirect semiconductors.[14]

However, for heavy-hole to spin-oribt band transitions, Eq. (2) is inadequate. It predicts that at energies both below the free-particle threshold ν_{th} and above the free-particle cutoff ν_c the absorption should vary as $\sim(\nu - E_g')^{-2}$ in qualitative disagreement with experiment. We have calculated the prediction of Landsberg theory using the RPA widths discussed later in this paper. The comparison with experiment is shown in Fig. 3.

C. Brinkman and Lee theory

A perturbation theoretic approach to line shapes has been explored by Brinkman and Lee.[7] They evaluate the correction to free particle theory to first order in the dynamically screened Coulomb potential. The free-particle theory for interband lineshapes can be represented in terms of a polarization graph as shown in Fig. 4. The dots represent coupling to photons, the double line represents the Green's function for band 1, the single line, the Green's function for band 2. Cutting the diagrams as shown by the dashed line represents taking the imaginary part of this polarization part with particles in bands 1 and 2 in initial or final states.

The corrections calculated by Brinkman and Lee[6] are shown in Fig. 5. Here the wiggly line represents the dynamically screened Coulomb interaction. Diagrams of type (a) to (c) admit of the simplest physical interpretation. They represent processes with a plasmon or single particle hole excitation in the final state. They can be interpreted as the square of the amplitudes shown in Fig. 6. The contribution to be added to the free-hole theory, Eq. (1), has the form

$$\Delta I_1^2(\hbar\nu) = \int d\hbar\omega\, d^3k_1\, d^3k_2[1-f^1(\epsilon_{\vec{k}_1}^1)]f^2(\epsilon_{\vec{k}_2}^2) \times \left|\frac{M_{\vec{k}_1}}{\hbar\nu + \epsilon_{\vec{k}_1}^1 - \epsilon_{\vec{k}_1}^2} + \frac{M_{\vec{k}_2}}{\epsilon_{\vec{k}_2}^2 - \hbar\nu - \epsilon_{\vec{k}_2}^1}\right|^2 \times \mathrm{Im}\left(\frac{V(q)}{\epsilon(q,\omega)}\right)\delta(\epsilon_{k_2}^1 + \hbar\nu - \epsilon_{k_2}^2 - \hbar\omega). \tag{3}$$

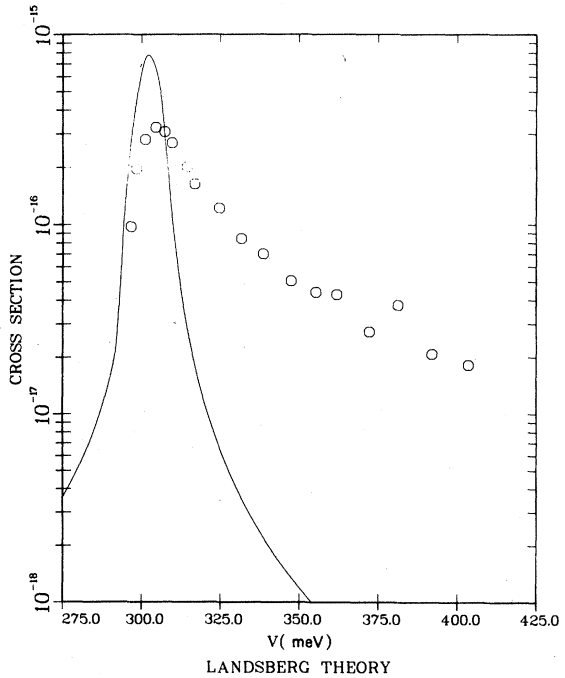

FIG. 3. Comparison between Landsberg theory and experiment for intervalence band transitions.

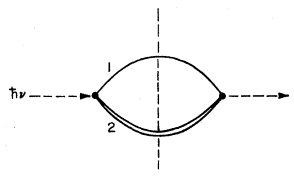

FIG. 4. Diagram for interband transitions in the free-particle theory for line shapes. The dot (●) denotes the coupling to photons. The dashed line cutting the diagram represents taking the imaginary part of this proper polarization graph to obtain the absorption. Particles in bands 1 and 2 are in the final state.

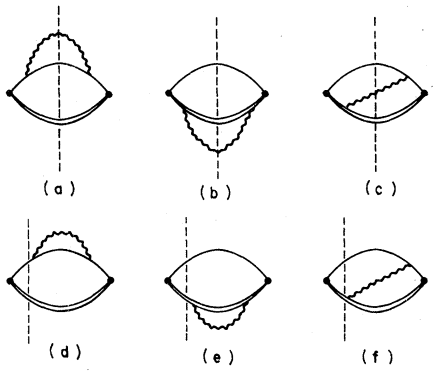

FIG. 5. Corrections to the free-particle theory considered by Brinkman and Lee. The wiggly line represents the dynamically screened Coulomb interaction. (a)–(c) Correspond to processes with plasmon or particle-hole excitations in the final state as well as particles in bands 1 and 2. (d)–(f) Processes where there are no plasmon or particle-hole excitations in the final state.

Here $\epsilon(q, \omega)$ is the dielectric function for the electron-hole plasma and $V(q)$ is the Coulomb potential.

The difficulty with Eq. (3) is that the denominators can be zero, yielding a divergent correction to the free-particle theory. Brinkman and Lee make a plasmon-pole approximation in which the true excitation spectrum of the electron hole plasma is replaced by a single high-frequency plasmon mode. This is often a good approximation because it is designed to satisfy the sum rules. For the problem which they treat, the gain spectrum of GaAs at moderate electron-hole densities, it is not possible in the plasmon pole approximation to satisfy simultaneously both the energy-conserving delta function and zero denominators. This is because the plasmon frequency is much greater than the sum of Fermi levels for electrons and holes. Therefore, they

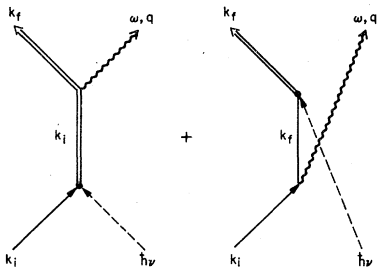

FIG. 6. Feynman diagrams for the amplitudes for interband transitions which when added and squared yield Figs. 5(a) to 5(c). The ω and q are the energy and momentum given to plasmon or particle-hole excitation. The k_i is the initial momentum of a particle in band 1, the k_f is the final momentum of a particle in band 2. The $\hbar\nu$ is the incident-photon energy.

obtain a nondivergent correction to the free-particle theory. However, this approximation becomes divergent as the density increases (or r_s decreases) in contrast to one's expectation of improved agreement with perturbation theory as the density increases. This is because the plasma frequency increases as $n^{1/2}$ while the Fermi levels increase as $n^{2/3}$, where n is the electron-hole pair density. Further, in the problem of heavy-hole to spin-orbit band absorption in electron-hole droplets in Ge, the parameters are such that (3) is divergent even in the plasmon-pole approximation. In all problems, Eq. (3) is divergent when the true excitation spectrum is used instead of the plasmon-pole approximation. The true excitation spectrum for electron-hole plasmas in zinc-blende semiconductors is discussed in Appendix A.

The other diagrams are also somewhat pathological. Diagrams 2(d) and 2(e) correspond to first-order terms in a self-energy insertion in the propagators. They diverge as the photon frequency approaches the threshold for the transition. Brinkman and Lee simply interpolate through the threshold region. Figure 2(f) corresponds to the first vertex correction. It is the term responsible for the enhancement factor. It is also divergent when the plasmon-pole approximation is replaced with the true spectrum.

III. QUALITATIVE PHYSICS OF HEAVY-HOLE TO SPIN-ORBIT BAND TRANSITIONS

The previous discussion has shown that the free hole theory and Landsberg theory[6] poorly describe the line shape for heavy-hole to spin-orbit band transitions. The Brinkman and Lee[7] perturbation approach is divergent for these transitions. Nevertheless, these theories are relevant to this problem since they can be shown to be limits of the more general theory which we now present. However, to motivate our approach we take the different starting point of multiple-scattering theory. The derivation presented below is not unique. The result can alternatively be obtained using ideas in formal transport and kinetic theory, as we intend to show in a future publication.[11]

A. Multiple-scattering approach

In their original work Pokrovsky and Svistunova[5] observed that the intervalence band absorption due to excitons and acceptor levels is similar to the measurements for electron-hole droplets. Smith, Chen, and McGill[15] have shown that the exciton intervalence band absorption measures the momentum spreading of the exciton wave function. In electron-hole droplets, as well as

in degenerately p-doped semiconductors, the screening is sufficiently large that bound states such as excitons or acceptor levels are absent. Our approach is to find an ansatz wave function appropriate to the limit where only scattering states are present.

Specifically, consider an idealized model of spherical heavy hole and spin-orbit split bands where the Coulomb potential acts only on particles in the heavy-hole band. Then, the absorption can be written schematically

$$\alpha(\hbar\nu) = \sum_i \int d^3k f(\epsilon_i^{\rm hh}) |M_{\vec{k}}|^2 |\langle \vec{k}|\psi_i\rangle|^2 \times \delta(\hbar\nu - \epsilon_{\vec{k}}^{\rm so} + \epsilon_i^{\rm hh}) . \quad (4)$$

Here the $|\psi_i\rangle$ are the wave functions for holes in the heavy-hole band, $|k\rangle$ is plane wave state, $M_{\vec{k}}$ is an interband matrix element, and the f is a statistical factor. For the free-hole theory the $|\psi_i\rangle$ are plane wave states and the sum over i runs over the momenta of holes in the heavy-hole band. For the exciton case, the $|\psi_i\rangle$ are exciton wave functions and i runs over the CM momenta of the excitons. For acceptor levels, the $|\psi_i\rangle$ are acceptor wave functions and i runs over the impurities. The problem, then, is the choice of $|\psi_i\rangle$ when only scattering states are present. First we consider the problem of the interband absorption in the presence of uncorrelated impurities which interact with holes via a highly screened but static potential V.

For the interaction of holes with a single impurity, the scattering wave function $|\psi_k^0\rangle$ would satisfy

$$\langle \vec{k}|\psi_{\vec{k}'}^0\rangle = (2\pi)^3\delta(\vec{k}-\vec{k}') - \frac{\langle \vec{k}|V|\psi_{k'}^0\rangle \exp[-i(\vec{k}-\vec{k}')\cdot\vec{r}]}{\epsilon_{\vec{k}}^{\rm hh} - \epsilon_{\vec{k}'}^{\rm hh} - i\epsilon}, \quad (5)$$

where $\vec{r}$ is the impurity position. When (5) is substituted into (4), one finds apart from forward scattering terms $\vec{k}=\vec{k}'$, a correction to be added to the free-hole theory

$$\Delta\alpha(\hbar\nu) = 2\int d^3k_i\, d^3k_f f(\epsilon_{\vec{k}_i}^{\rm hh}) \left| \frac{M_{\vec{k}_f}\langle \vec{k}_f|V|\psi_{\vec{k}_i}^0\rangle}{\epsilon_{\vec{k}_f}^{\rm hh} - \epsilon_{\vec{k}_f}^{\rm so} + \hbar\nu - i\epsilon} \right|^2 \times \delta(\hbar\nu - \epsilon_{\vec{k}_f}^{\rm so} + \epsilon_{\vec{k}_i}^{\rm hh}) . \quad (6)$$

In the Born approximation $\langle \vec{k}|V|\psi_{\vec{k}'}^0\rangle \simeq \langle \vec{k}|V|\vec{k}'\rangle$, Eq. (6) is the lowest-order correction to the free-hole theory. It is also the impurity scattering analog of the square of the diagram in Fig. 6(b) of the Brinkman and Lee theory.[7] Note that at $\nu_{\rm th} < \nu < \nu_c$, where $\nu_{\rm th}$ and ν_c are identified in Fig. 1, Eq. (6) is divergent because the denominator $\epsilon_{\vec{k}_f}^{\rm hh} - \epsilon_{\vec{k}_f}^{\rm so} + \hbar\nu$ can be zero as in the Brinkman and Lee theory. However, for high frequencies $\nu \gg \nu_c$, where the denominator is nonzero because of the Fermi function f, (6) should be the valid perturbation correction.

For our system of uncorrelated impurities, we must find a wave function which preserves the high-frequency result, is finite at $\nu < \nu_c$, and recovers the free-particle result in the weak scattering limit $V \to 0$. Our choice is motivated by the idea of a coherent wave in multiple-scattering theory and by the extinction theorem.[16] The coherent wave idea is that a plane wave propagating through a system of uncorrelated scatterers is attenuated and the effective wave vector shifted. The result is the addition to the energy $\epsilon_{\vec{k}}$ of a self-energy $\Sigma(\vec{k})$ related to the forward scattering amplitude by $n_I\langle k|V|\psi_{\vec{k}}^0\rangle$, where n_I is the impurity density. That this produces the correct attenuation can be obtained from the optical theorem

$$\mathrm{Im}\langle \vec{k}|V|\psi_{\vec{k}}^0\rangle = -\frac{mk}{2\pi\hbar^2}\int \frac{d\Omega_{\vec{k}'}}{4\pi}\left|\langle \vec{k}|V|\psi_{\vec{k}'}^0\rangle\right|^2; \quad |\vec{k}| = |\vec{k}'| . \quad (7)$$

The extinction theorem states that in an infinite system the free-particle part [the $(2\pi)^3\delta(\vec{k}-\vec{k}')$ in Eq. (5)] must be completely cancelled by the scattered waves. The following ansatz wave function satisfies the extinction theorem

$$\langle \vec{k}|\psi_{\vec{k}'}^M\rangle \equiv (2\pi)^3\delta(\vec{k}-\vec{k}') - \sum_j \frac{\exp[i(\vec{k}-\vec{k}')\cdot\vec{r}_j]\langle \vec{k}|V|\psi_{\vec{k}'}^0\rangle}{\epsilon_{\vec{k}} + \Sigma(k) - \epsilon_{\vec{k}'}} . \quad (8)$$

The proof of this and other arguments in this section may be obtained in Appendix B.

We now substitute the wave function (8) into (4) and impurity average. As shown in Appendix B, the parts which are singular as $\vec{k}\to\vec{k}'$ exactly cancel with the result

$$\alpha(\hbar\nu) \simeq 2n_I \int \frac{d^3k_i}{(2\pi)^3} f(\epsilon_{\vec{k}_i}^{\rm hh}) \times \int \frac{d^3k_f}{(2\pi)^3} \frac{|M_{\vec{k}_f}|^2 |\langle \vec{k}_f|V|\psi_{\vec{k}_i}^0\rangle|\ \delta(\hbar\nu - \epsilon_{\vec{k}_f}^{\rm so} + \epsilon_{\vec{k}_i}^{\rm hh})}{\left[\epsilon_{\vec{k}}^{\rm hh} + \Sigma^{\rm hh}(\vec{k}_f) - \epsilon_{\vec{k}}^{\rm so} + \hbar\nu\right]^2} . \quad (9)$$

Now we note several remarkable properties of Eq. (9). First in the limit $\Sigma(\vec{k}_f)\to 0$, Eq. (9) is the lowest-order perturbation correction, Eq. (6), to be added to the free-hole theory. Second, at high frequencies $\nu \gg \nu_c$ it reproduces the perturbation result. Third, at low frequencies $\nu < \nu_c$, (9) is convergent. Fourth, in the limit of weak scattering or low densities of impurities (9) reduces to the free hole theory. This last statement is easily proved with the aid of the optical theorem, Eq. (7). Moreover, explicit calculation of (9) with, for example, a screened Yukawa po-

tential shows that it reproduces the characteristics of the data. This includes a peak at low frequencies close to the free-hole theory and a slowly decreasing tail at high frequencies. This calculation is shown in Ref. 10 for various values of screening. We take $M_{\vec{k}_f} \sim kM$ which is the low-k dependence of the matrix element for interband transitions as shown in the Appendix A. Thus, the multiple-scattering ansatz wave function, Eq. (8), already contains the principal effects associated with the line shape for heavy hole to spin-orbit band transitions. It also shows clearly the relation of the line shapes of excitons and acceptor levels to the results for electron-hole droplets.

B. Extension to electron-hole droplets and the random-phase approximation

In going from impurity systems to electron-hole droplets the principal effect is to change from scattering off impurities to scattering off the elementary excitations of the electron-hole plasma. We shall turn Eq. (9) into the electron-hole droplet result by pointing out how the various quantities in (9) are transformed in going from impurities to excitations. The formulas below apply only at $T = 0$ °K. The finite temperature generalization will be discussed elsewhere.

Unlike impurities, elementary excitations can also take up energy $\hbar\omega$. Thus, the statically screened potential should go to the dynamically screened potential:

$$|V(q)|^2 \to \frac{|V(q)|^2}{|\epsilon(q,\omega)|^2}, \tag{10}$$

where $\epsilon(q,\omega)$ is the dielectric function of the electron-hole plasma and $V(q)$ is the Coulomb potential. The impurity density n_I should go to the density of elementary excitations

$$n_I \to 2\sum_i \int d\hbar\omega \int \frac{d^3k}{(2\pi)^3} f^i(k) \times [1 - f^i(k+q)]\delta(\hbar\omega + \epsilon_k^i - \epsilon_{k+q}^i), \tag{11}$$

where i denotes each component of the plasma. This in turn is related to the imaginary part of the dielectric function

$$n_I \to \int d\hbar\omega \frac{1}{V(q)} \frac{\epsilon^I(q,\omega)}{\pi}. \tag{12}$$

The coherent-wave self-energy must go to the self-energy due to scattering off elementary excitations. This is given by the random-phase-approximation self-energy. The imaginary part of the RPA self-energy may be written

$$\Sigma^I(k) = \frac{2\pi}{\hbar}\int \frac{d^3q}{(2\pi)^3}\int \frac{d\hbar\omega}{\pi} \mathrm{Im}\left(\frac{V(q)}{\epsilon(q,\omega)}\right)\delta(\epsilon_k - \epsilon_{k'} \pm \hbar\omega) \times \Theta(\pm(\epsilon_F - \epsilon_{k'})); \quad q = k - k', \tag{13}$$

where ± signs refer to particles below or above the Fermi surface, respectively. The energy-conserving δ function in (9) must allow for the fact that energy can be given to the elementary excitations:

$$\delta(\hbar\nu - \epsilon_{k_f}^{so} + \epsilon_{k_i}^{hh}) \to \delta(\hbar\nu - \epsilon_{k_f}^{so} + \epsilon_{k_i}^{hh} - \hbar\omega). \tag{14}$$

Here we assume that the real part of the self-energy produces a rigid-band shift. Finally, one should relax the assumption made in deriving (9) that scattering only occurs in the heavy-hole band. Thus, allowing for scattering in the spin-orbit-split band, one has

$$\left|\frac{M_{k_f}}{\epsilon_{k_f}^{hh} + \Sigma^{hh}(k_f) - \epsilon_{k_f}^{so} + \hbar\nu}\right|^2 \to \left|\frac{\vec{k}_f M}{\epsilon_f^{hh} + \Sigma_f^{hh} + \hbar\nu - \epsilon_f^{so} - \Sigma_f^{so}} - \frac{\vec{k}_i M}{\epsilon_i^{hh} + \Sigma_i^{hh} + \hbar\nu - \epsilon_i^{so} - \Sigma_i^{so}}\right|^2. \tag{15}$$

Here, the two terms in Eq. (15) correspond to the two diagrams in Fig. 6, and we again take $M_{k_f} \sim k_f M$ appropriate to interband transitions.

Putting all this together, the final schematic expression for the intervalence band absorption has the form

$$\alpha(\hbar\nu) \propto 2\int \frac{d^3k_i\, d^3k_f}{(2\pi)^6}\int_0^\infty \frac{d\hbar\omega}{\pi}\left|\frac{\vec{k}_f M}{\epsilon_f^{hh} + \Sigma_f^{hh} - \epsilon_f^{so} - (\Sigma_f^{so})^* + \hbar\nu} - \frac{\vec{k}_i M}{\epsilon_i^{hh} + \Sigma_i^{hh} + \hbar\nu - \epsilon_i^{so} - (\Sigma_i^{so})^*}\right|^2 \times f(\epsilon_i^{hh})\,\mathrm{Im}\left(\frac{V(q)}{\epsilon(q,\omega)}\right)\delta(\hbar\nu + \epsilon_i^{hh} - \epsilon_f^{so} - \hbar\omega), \tag{16}$$

where the asterisk denotes complex conjugate. Note that this form is quite similar to the Brinkman-Lee expression for the correction to the free-hole theory. However, Eq. (16) is convergent at all frequencies. It includes the free-hole theory which becomes the dominant contribution in the limit of small r_s (or high density). This can be proved with the aid of (13). Further,

Eq. (16) may be reduced to the Landsberg theory. For example, in the first term in (1) simply assume the self-energies are sufficiently small in the denominators that $-\epsilon_f^{so}+\hbar\nu$ in the δ function should be replaced by ϵ_f^{hh}. Then, using (13), the Landsberg theory follows.

IV. COMPARISON TO EXPERIMENT

A. Spherical-model calculations

In order to compare our theory with experiment, it is necessary to take into account detailed effects of the band structure in germanium. Properties of the spherical model for $\vec{k}\cdot\vec{p}$ valence band Hamiltonian relevant to the present study are worked out in Appendix A. Of significance are the electromagnetic (em) coupling matrix elements, and the nonparabolicity of the spin-orbit band. Combining the theory of the preceding section with the results in Appendix A, and after summing over the photon polarizations, one obtains the cross section for heavy-hole to spin-orbit band transitions

$$\sigma_{hh\to so}=\frac{3\mu^2\hbar^2\gamma_1^2e^2}{n_h c m_0^2\nu\sqrt{\epsilon_0}\,32\pi^5}\int d^3k_i\,d^3k_f\,d\hbar\omega f(\epsilon_i^h)\,\mathrm{Im}\left(\frac{V(q)}{\epsilon(q,\omega)}\right)\delta(\hbar\nu+\epsilon_i^h-\epsilon_f^{so}-\hbar\omega)$$
$$\times\left|\frac{\vec{k}_i x_i^*}{\hbar\nu+\epsilon_i^h+\Sigma_i^h-\epsilon_i^{so}-{}^*\Sigma_i^{so}}+\frac{\vec{k}_f x_f^*}{\epsilon_f^{so}+{}^*\Sigma_f^{so}-\hbar\nu-\epsilon_f^h-\Sigma_f^h}\right|^2. \tag{17}$$

Here μ and γ_1 are spherical model parameters of Baldereschi and Lipari, n_h is the electron-hole pair density in electron-hole droplets, and x^* are k-dependent matrix elements given in Eq. (A10). The parameters of electron-hole droplets used in our calculations are the same as given for Ge in Ref. 1.

In carrying out calculations the following additional assumptions are made: (i) it is assumed that the real part of the self-energy produces only a rigid band shift;[17] (ii) the dielectric function is taken in the spherical model for holes and in a spherical approximation with density-of-states mass for electrons. However, we retain the full effects of the damping of plasmons by heavy-hole to light-hole transitions in the imaginary part of the dielectric function. A more complete discussion of the dielectric function is given in Appendix A; (iii) we ignore contributions from the light-hole band since only ~5% of holes are in this band. In addition, Eq. (17) explicitly assumes that vertex corrections can be ignored or are constant in energy, and it assumes that only single-plasmon or particle-hole excitations are important. These approximations will be discussed in more detail in Sec. V C.

In these spherical approximations our results for the imaginary parts of the RPA self-energies calculated from Eq. (13) are shown in Fig. 7 for the heavy-hole band and in Fig. 8 for the spin-orbit-split band. The imaginary part of the heavy-hole self-energy goes to zero at the Fermi surface. These self-energies were used in the comparison of experiment and Landsberg theory shown in Fig. 3.

A comparison between our results for the cross section for heavy-hole to spin-orbit band transitions and experiment is shown as the solid line in Fig. 9. We note that the high-frequency tail is in excellent agreement with experiment both with regard to slope and normalization (however, the normalization of experiment is somewhat uncertain). The very high frequency results are also independent of the choice of dielectric function such as the Hubbard or Singwi modifications.[19] This is because the high-frequency cross section

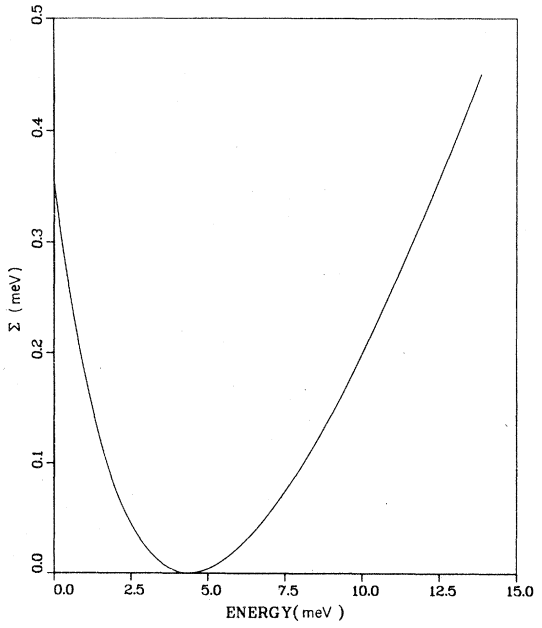

FIG. 7. Imaginary part of the heavy-hole self-energy calculated in the RPA and the spherical approximation to the valence-band structure.

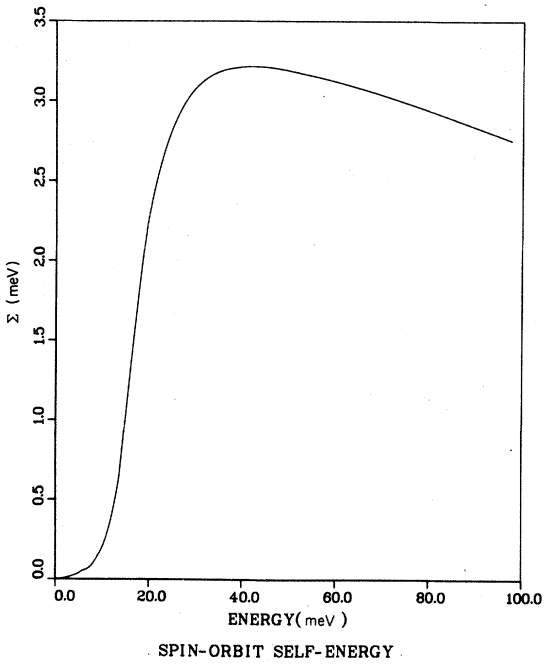

FIG. 8. Same as Fig. 7 for the imaginary part of the spin-orbit-split band self-energy.

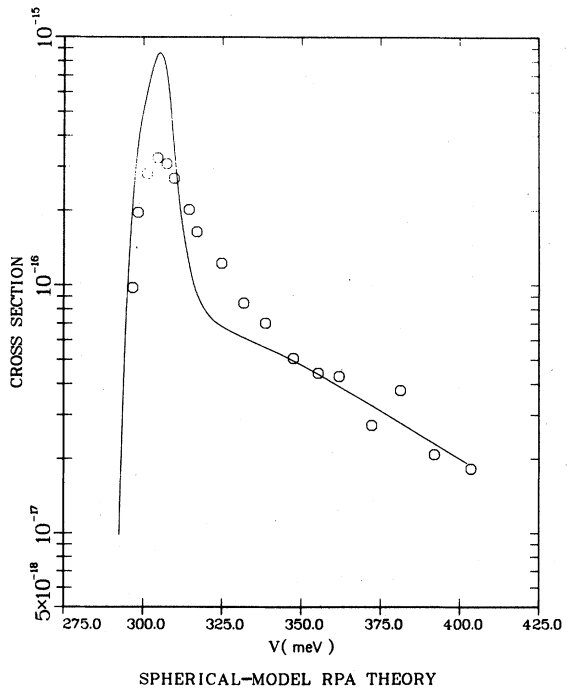

FIG. 9. Comparison between our multiple-scattering RPA theory and experiment for heavy-hole to spin-orbit-split band transitions. The spherical model for the valence-band structure was assumed.

is the result of scattering at large momentum transfers where screening is unimportant. At low frequencies our results exceed experiment and are close to the free hole theory for the spherical model shown as the dashed line in Fig. 1. It is clear from Fig. 1 that much of the discrepancy between the spherical-model RPA and experiment can be removed by taking into account the mass anisotropy of the heavy-hole band. This is discussed in Sec. IV B. At intermediate frequencies calculations show that the results are somewhat sensitive to the choice of dielectric function as might be expected to be important at moderate momentum transfers. This is discussed further in Sec. IV C.

Our results are also quite sensitive to band coupling effects due to the finite spin-orbit splitting as discussed in Appendix A. The long-dashed curve in Fig. 10 shows the result of keeping the matrix element x_+ and the spin orbit mass at their $k=0$ values. The short-dashed line keeps the $k=0$ value of x_+ but allows the spin-

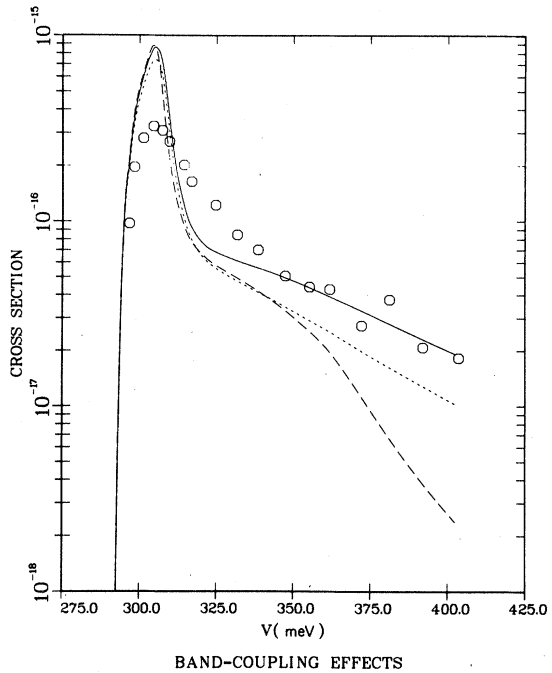

FIG. 10. Band-coupling effects on the heavy-hole to spin-orbit split-band transitions calculated in the spherical model. The long-dashed line shows the effect of assuming a parabolic spin-orbit-split band and assuming that the em coupling matrix elements are momentum independent. The short-dashed line includes the nonparabolicity but retains the constant matrix elements. The solid line is the complete calculation including the full band-coupling effects. The circles are the experiment of Pokrovsky and Svistunova.

orbit band to be nonparabolic. Finally, the solid line is again the full calculation. We note that $|x_+|^2$ increases by a factor of 3 between $k=0$ and large k. In their calculation on the exciton line shape, Smith *et al.*[15] ignore the k dependence of this matrix element and obtained a cross section which was low by a factor of about 2 at $\nu - \nu_{th} \simeq 100$ meV.

B. Nonspherical-model calculations

In order to study the effects of mass anisotropy, we have carried out Monte Carlo evaluations of the six-dimensional integrals in Eq. (17) with ϵ_i^h evaluated with a fully anisotropic effective mass. The hole contribution to the dielectric function and the matrix elements were still in the spherical model. We found that the anisotropy of the electron effective mass while large had little effect on our calculated cross sections. In order to evaluate (17) we first had to determine the anisotropy of the heavy-hole self-energies. The results for the [100] and [111] directions are shown in Fig. 11. We note that below the Fermi level the effects of mass anisotropy were small. These calculations of self-energy were then fit with zeroth and first cubic harmonics in evaluating Eq. (17).

The results of this calculation are shown in Fig. 12. The theoretical points have error bars indicating the variance of the Monte Carlo calculations. As expected, the effect of mass anisotropy is to considerably improve the agreement between experiment and theory at low frequencies. However, the theory is still somewhat above the experiment. Possible reasons for this discrepancy are discussed qualitatively in Sec. IV C. At high frequencies the mass anisotropy has little effect on the calculated cross section, and the good agreement with experiment is retained.

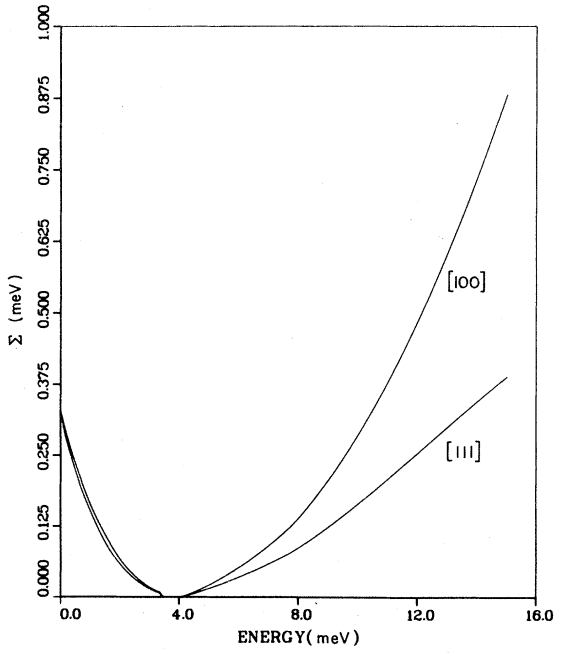

HEAVY-HOLE SELF-ENERGY

FIG. 11. Imaginary part of the heavy-hole self-energy calculated using the full mass anisotropy of the true band structure.

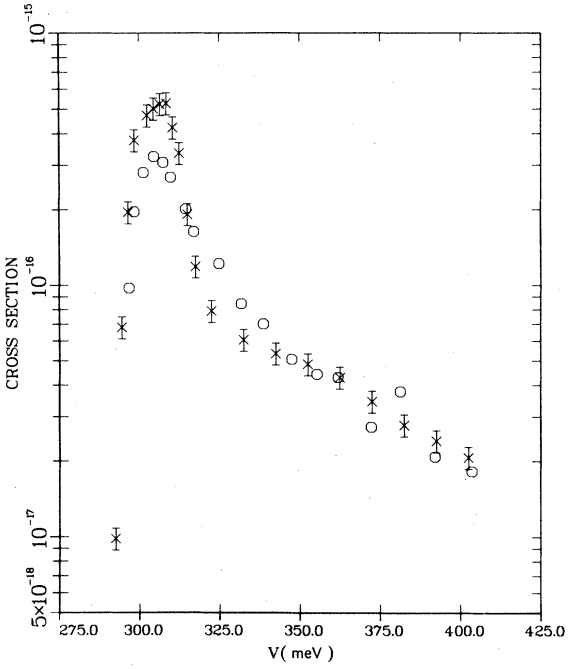

NONSPHERICAL-MODEL RPA THEORY

FIG. 12. Comparison between Monte Carlo integrations of our multiple-scattering RPA theory using the full band-structure anisotropy (✕) and experiment (○) for heavy-hole to spin-orbit-split band transitions. The errors on the theoretical points represent the variance of the Monte Carlo calculations.

C. Qualitative discussion of additional effects

Our best calculation, Fig. 12, is somewhat more strongly peaked at low frequencies than the experiment. There are several effects which are not included within the present theory which might qualitatively explain the discrepancy. These are the dispersion of the self-energy, local field and exchange corrections to the dielectric function, and vertex corrections.

Our calculation assumes that the effect of the real part of the self energy is to rigidly shift the bands. This is known to be accurate to within 10% for electrons and holes below their Fermi levels.[17] However, for the spin-orbit-split band

the experiment varies between energies near threshold where the real part of the self-energy is minus several meV to high energies where the real part of the self-energy should be negligible. This is because the electron-hole plasma can respond fast enough to screen a low-energy particle but cannot respond fast enough to screen a high-energy particle. The biggest change should occur around a plasmon energy (~13 meV) above the bottom of the spin-orbit-split band. Qualitatively, inclusion of this effect will act to broaden the low-frequency peak and, thereby, improve agreement with experiment.

Our calculation also took the simplest possible form of the RPA dielectric function which in effect amounted to ignoring local field and exchange corrections. A number of authors have proposed modified RPA dielectric functions which are claimed to give more accurate results at larger r_s (lower densities). Let $Q(q,\omega)=V(q)\Pi^0(q,\omega)$, where $\Pi^0(q,\omega)$ is the zeroth-order proper polarization. Then in our problem, introduction of local field and exchange corrections would amount to the replacement[19]

$$\mathrm{Im}\left(\frac{1}{\epsilon}\right)=\frac{Q_0^I}{(1-Q_0^R)^2+(Q_0^I)^2} \rightarrow \frac{Q_0^I}{\{1-[1-G(q)]Q_0^R\}^2+\{[1-G(q)]Q_0^I\}^2}, \tag{18}$$

where $G(q)$ is positive definite and is zero at $q=0$. It is obvious that these corrections increase the amount of scattering. Therefore, they act to broaden the calculated cross section at low frequencies improving the agreement with experiment. At high frequencies where screening is unimportant the good agreement with experiment will be retained.

Finally, our calculation assumed that the vertex correction was either negligible or constant in energy. Qualitatively, there is an attractive interaction between a hole in the spin-orbit-split band and an electron in the heavy-hole band. Because of the difference in effective masses, this interaction is weaker than the interaction between an electron in the conduction band and a hole in the valence band which leads to an enhancement factor of 2 to 3 for EHD luminescence. More importantly, the matrix element coupling the valence bands is proportional to momentum. In a spherical approximation, the heavy-hole to spin-orbit band transitions are in a relative $l=1$ angular-momentum state. The effect of the attractive interaction is reduced by the angular-momentum barrier. Thus, vertex corrections are expected to be less important than in EHD luminescence.

Thus, we believe that the remaining discrepancies between our calculations and experiment on the line shape for heavy-hole to spin-orbit-split band transitions can be explained within the RPA which has been successful for thermodynamic properties.

V. CONCLUSIONS AND DISCUSSION

We have presented a new approach for calculating the effects of scattering processes on the line shapes for electron-hole plasmas in semiconductors. It provides the first explanation of the broad line shape for absorption due to heavy-hole to spin-orbit-split band transitions observed in electron-hole droplets in Ge. The line shape may be understood within the random phase approximation which has previously been successful for thermodynamic properties. The line shape is also sensitive to details of the valence-band structure of Ge, which we have derived for the spherical approximation in Appendix A.

The theory of this paper should also be applicable to a variety of other transitions where deviations from free-particle theories are observed. We have carried out detailed calculations[24] for EHD luminescence in the indirect semiconductor Si. The calculations are close to the free-particle theory at energies above the free-particle threshold. This is expected since additional momentum nonconservation due to scattering from the elementary excitations of the plasma should not strongly affect line shapes where momentum is already not conserved because of phonon scattering. The calculations have a weak, slowly decreasing tail at energies below the free-particle threshold in agreement with experiment. Calculations are currently in progress[25] on the gain spectra of direct-gap semiconductors where strong departures from the free-particle theories have been observed. In both these problems there is a large gap between bands. It is somewhat more complex to deal with degenerate bands as in the heavy-hole to light-hold absorption responsible for the plasmon width in EHD. We expect to report results on these problems in future publications.

The arguments of this paper have been largely intuitive. It is also possible to provide a formal derivation of our results using ideas in transport and kinetic theory. This derivation should lead to a more complete theory in which assumptions made in the present calculations can be relaxed. These include the assumption that the bands are rigidly shifted by the many body interactions, and the assumption that enhancement factors (vertex corrections) are either constant in energy or negligible. This will be addressed in a separate publication.[11]

ACKNOWLEDGMENTS

The authors thank D. F. DuBois, J. E. Gubernatis, and R. B. Hammond for many helpful discussions.

APPENDIX A: SPHERICAL MODEL FOR FINITE SPIN-ORBIT SPLITTING

In this Appendix, we present details of the analysis of the spherical model for the $\vec{k}\cdot\vec{p}$ valence band Hamiltonian of diamond and zinc-blende semiconductors. The quantities discussed include the band-structure nonparabolicity, the em coupling matrix elements, the free-particle dielectric function, and the matrix elements of the potential. As discussed in the main text, all of these quantities enter in essential ways into the calculation of the absorption due to transitions between heavy-hole and spin-orbit bands. It is also useful to collect these results for reference in further papers by the authors to follow on line shape problems in diamond and zinc-blende semiconductors.

The spherical model has been discussed previously by Combescot and Nozières[20] and by Rose and Shore[21] in the limit of infinite spin-orbit splitting. Our discussion of the band coupling effects due to the finite spin-orbit splitting is motivated by the large size of these effects on the absorption due to heavy-hole to spin-orbit transitions.

The spherical model is obtained from the general kp Hamiltonian by setting to zero the cubic anisotropy parameter δ of Baldereschi and Lipari.[18] This is equivalent to approximating the L, M, and N of the original paper by Kane[22] by

$$L=\frac{\hbar^2\gamma_1(1+2\mu)}{2m_0};\quad M=\frac{\hbar^2\gamma_1(1-\mu)}{2m_0};\quad N=\frac{\hbar^2\gamma_1 3\mu}{2m_0}, \tag{A1}$$

where γ_1 and μ are defined and tabulated for various semiconductors by Baldereschi and Lipari. Thus, including the spin-orbit splitting Δ, the $\vec{k}\cdot\vec{p}$ Hamiltonian in the $|x\uparrow\rangle\,|y\uparrow\rangle\,|z\uparrow\rangle\,|x\downarrow\rangle\,|y\downarrow\rangle\,|z\downarrow\rangle$ basis is

$$\frac{2m}{\hbar^2\gamma_1}H=\begin{array}{c} \\ |x\uparrow\rangle \\ |y\uparrow\rangle \\ |z\uparrow\rangle \\ |x\downarrow\rangle \\ |y\downarrow\rangle \\ |z\downarrow\rangle \end{array}\begin{array}{c} \begin{array}{cccccc} |x\uparrow\rangle & |y\uparrow\rangle & |z\uparrow\rangle & |x\downarrow\rangle & |y\downarrow\rangle & |z\downarrow\rangle \end{array} \\ \begin{pmatrix} (1+2\mu)k_x^2 & 3\mu k_x k_y & 3\mu k_x k_z & 0 & 0 & -\tfrac{1}{3}\tilde{\Delta} \\ +(1-\mu)(k_y^2+k_z^2) & +\tfrac{1}{3}i\tilde{\Delta} & & & & \\ 3\mu k_x k_y & (1+2\mu)k_y^2 & 3\mu k_y k_z & 0 & 0 & \tfrac{1}{3}i\tilde{\Delta} \\ -\tfrac{1}{3}i\tilde{\Delta} & +(1-\mu)(k_x^2+k_z^2) & & & & \\ 3\mu k_x k_z & 3\mu k_y k_z & (1+2\mu)k_z^2 & \tfrac{1}{3}\tilde{\Delta} & -\tfrac{1}{3}i\tilde{\Delta} & 0 \\ & & +(1-\mu)(k_x^2+k_y^2) & & & \\ 0 & 0 & \tfrac{1}{3}\tilde{\Delta} & (1+2\mu)k_x^2 & 3\mu k_x k_y & 3\mu k_x k_z \\ & & & +(1-\mu)(k_y^2+k_z^2) & -\tfrac{1}{3}i\tilde{\Delta} & \\ 0 & 0 & \tfrac{1}{3}i\tilde{\Delta} & 3\mu k_x k_y & (1+2\mu)k_y^2 & 3\mu k_y k_z \\ & & & +\tfrac{1}{3}i\tilde{\Delta} & +(1-\mu)(k_x^2+k_z^2) & \\ -\tfrac{1}{3}\tilde{\Delta} & -\tfrac{1}{3}i\tilde{\Delta} & 0 & 3\mu k_x k_z & 3\mu k_y k_z & (1+2\mu)k_z^2 \\ & & & & & +(1-\mu)(k_x^2+k_y^2) \end{pmatrix} \end{array}, \tag{A2}$$

$$\tilde{\Delta}=2m_0\Delta/\hbar^2\gamma_1 k^2. \tag{A3}$$

Define

$$\lambda_\pm=\tfrac{1}{2}(2+\mu+\tilde{\Delta})\pm\tfrac{1}{2}(9\mu^2-2\tilde{\Delta}\mu+\tilde{\Delta}^2)^{1/2}. \tag{A4}$$

Then the Hamiltonian may be diagonalized with eigenvalues

$$\epsilon_{hh}=\frac{\hbar^2k^2\gamma_1(1-\mu)}{2m_0},\quad \epsilon_{lh}=\frac{\hbar^2k^2\gamma_1\lambda_-}{2m_0},\quad \epsilon_{so}=\frac{\hbar^2k^2\gamma_1\lambda_+}{2m_0}. \tag{A5}$$

Thus, the heavy-hole band is parabolic in the spherical model while both light-hole and spin-

orbit bands have nonparabolic dispersion relations. The small-k limit is

$$\epsilon_{\rm lh} = \frac{\hbar^2 k^2 \gamma_1 (1+\mu)}{2m_0}, \quad \epsilon_{\rm so} = \Delta + \frac{\hbar^2 k^2 \gamma_1}{2m_0}. \tag{A6}$$

The large-k limit is

$$\epsilon_{\rm lh} = \frac{\hbar^2 k^2 \gamma_1 (1-\mu)}{2m_0}, \quad \epsilon_{\rm so} = \Delta + \frac{\hbar^2 k^2 (1+2\mu)}{2m_0}. \tag{A7}$$

The nonparabolicity of the spin-orbit band is quite important to the calculation of the main text as shown in Fig. 10.

The eigenvectors may be written in terms of Bloch functions

$$\phi_{k\lambda} = \sum_j e^{i\vec{k}\cdot\vec{r}} b_j^\lambda u_j e^{-i\omega_k^\lambda t}, \tag{A8}$$

where λ labels the eigenstates, $\hbar\omega_k^\lambda$ denotes the eigenenergies (A5), and the b_j^λ may be written for k in the z direction as

$$|\,\mathrm{hh}\uparrow\rangle = \begin{pmatrix} 1/\sqrt{2} \\ i/\sqrt{2} \\ 0 \\ 0 \\ 0 \\ 0 \end{pmatrix} \quad |\,\mathrm{hh}\downarrow\rangle = \begin{pmatrix} 0 \\ 0 \\ 0 \\ 1/\sqrt{2} \\ -i/\sqrt{2} \\ 0 \end{pmatrix}$$

$$|\,\mathrm{lh,so}\uparrow\rangle = \begin{pmatrix} y_\pm \\ -iy_\pm \\ 0 \\ 0 \\ 0 \\ x_\pm \end{pmatrix} \quad |\,\mathrm{lh,so}\downarrow\rangle = \begin{pmatrix} 0 \\ 0 \\ x_\pm \\ -y_\pm \\ -iy_\pm \\ 0 \end{pmatrix}, \tag{A9}$$

where

$$y_\pm = \frac{\frac{1}{3}\tilde{\Delta}}{[(1-\mu-\lambda_\pm+\frac{2}{3}\tilde{\Delta})^2 + 2(\frac{1}{3}\tilde{\Delta})^2]^{1/2}},$$

$$x_\pm = \frac{1-\mu-\lambda_\pm+\frac{2}{3}\tilde{\Delta}}{[(1-\mu-\lambda_\pm+\frac{2}{3}\tilde{\Delta})^2 + 2(\frac{1}{3}\tilde{\Delta})^2]^{1/2}}, \tag{A10}$$

where (+) and (−) refer to the spin-orbit and light-hole bands, respectively, as defined in (A4). The eigenvectors for k in arbitrary directions may be obtained by the application of the appropriate rotation matrices to (A9). This is done most readily be expressing these states in a J, J_z representation as follows:

$$|\,\mathrm{hh}\rangle = |\,\tfrac{3}{2},\tfrac{3}{2}\rangle; \quad |\,\tfrac{3}{2},-\tfrac{3}{2}\rangle,$$
$$|\,\mathrm{so}\rangle = (\tfrac{2}{3})^{1/2}(x_+ + y_+)|\,\tfrac{3}{2},\pm\tfrac{1}{2}\rangle + \frac{2y_+ - x_+}{\sqrt{3}}|\,\tfrac{1}{2},\pm\tfrac{1}{2}\rangle,$$
$$|\,\mathrm{lh}\rangle = (\tfrac{2}{3})^{1/2}(x_- + y_-)|\,\tfrac{3}{2},\pm\tfrac{1}{2}\rangle + \frac{2y_- - x_-}{\sqrt{3}}|\,\tfrac{1}{2},\pm\tfrac{1}{2}\rangle. \tag{A11}$$

Then, to rotate these to a new $\vec{k}$ direction, use the $d^J_{j_z j'_z}(\theta)$ representations of the rotation group.

The dielectric function is obtained from the response function

$$\Pi(q,\omega) = \frac{1}{i\hbar}\int d^3(x-x')\,d(t-t')\,e^{-iq(x-x')} \times e^{i\omega(t-t')}\langle 0|\,T(\hat{n}(x,t)\hat{n}(x',t'))|\,0\rangle, \tag{A12}$$

where the density $\hat{n}(x,t) = \hat{\psi}^\dagger(x,t)\hat{\psi}_\lambda(x,t)$ is given in terms of

$$\hat{\psi}(x,t) = \sum_\lambda \int \frac{d^3k}{(2\pi)^3}\hat{a}_{k\lambda}\phi_{k\lambda}\,e^{i\vec{k}\cdot\vec{r}}e^{-i\omega_k^\lambda t}, \tag{A13}$$

where $\hat{a}_{\beta\lambda}$ is an annihilation operator. Thus, one obtains

$$\Pi(q,\omega) = \sum_{\lambda_1\lambda_2}\frac{d^3k}{(2\pi)^3}(1-n_{k+q}^{\lambda_1})n_k^{\lambda_2}|\,M_{\lambda_1\lambda_2}|^2 \times\left(\frac{1}{\hbar\omega-\hbar(\omega_{k+q}^{\lambda_1}-\omega_k^{\lambda_2})+i\epsilon} - \frac{1}{\hbar\omega+\hbar(\omega_{k+q}^{\lambda_1}-\omega_k^{\lambda_2})-i\epsilon}\right), \tag{A14}$$

where the $M_{\lambda_1\lambda_2}$ are the matrix elements of the rotated Bloch functions (A8) depending on the angle θ between $\vec{k}$ and $\vec{k}+\vec{q}$. For example,

$$M^{\vec{k},\vec{k}+\vec{q}}_{\mathrm{hh}\uparrow,\mathrm{so}\uparrow} = (\tfrac{2}{3})^{1/2}(x_+^{(k+q)} + y_+^{(k+q)})\,d^{3/2}_{3/2,1/2}(\theta).$$

Working this out one finds that for transitions between bands 1 and 2 the contribution to the response function is

$$\Pi_{12}(q,\omega) = 2\int\frac{d^3k}{(2\pi)^3}T^{12}_{k,k+q}(1-n_{k+q}^1)n_k^2 \times\left(\frac{1}{\hbar\omega-\hbar(\omega_{k+q}^1-\omega_k^2)+i\epsilon} - \frac{1}{\hbar\omega+\hbar(\omega_{k+q}^1-\omega_k^2)-i\epsilon}\right), \tag{A15}$$

where

$$T^{\mathrm{hh,hh}}_{k,k+q} = \tfrac{1}{4}+\tfrac{3}{4}\cos^2\theta_{k,k+q},$$
$$T^{\mathrm{hh,lh\,(so)}}_{k,k+q} = \tfrac{2}{3}(x_\mp^{(k+q)}+y_\mp^{(k+q)})^2\tfrac{3}{4}\sin^2\theta_{k,k+q},$$
$$T^{\mathrm{lh,lh}}_{k,k+q} = \tfrac{2}{3}(x_-^k+y_-^k)(x_-^{k+q}+y_-^{k+q})[\tfrac{1}{2}(3\cos\theta-1)]^2 + \tfrac{1}{3}[(2y_-^k-x_-^k)(2y_-^{k+q}-x_-^{k+q})],$$
$$T^{\mathrm{lh,so}}_{k,k+q} = \tfrac{2}{3}(x_-^k+y_-^k)(x_+^{k+q}+y_+^{k+q})[\tfrac{1}{2}(3\cos\theta-1)]^2 + \tfrac{1}{3}[(2y_-^k-x_-^k)(2y_+^{k+q}-x_+^{k+q})]. \tag{A16}$$

From these expressions the optical cross section per hole may be obtained by taking the $q \to 0$ limit with

$$\sigma = \frac{\omega}{c n_h} \frac{\epsilon_I(0,\omega)}{\sqrt{\epsilon_R}}, \tag{A17}$$

where ϵ_R and ϵ_I are real and imaginary parts of the dielectric function, and n_h is the hole density.

The same answer for the optical cross section can be alternatively obtained by using the (A9) to calculate the matrix element of the electromagnetic Hamiltonian between bands. In the $|x\rangle, |y\rangle, |z\rangle$ basis for k in the z direction the terms linear in the vector potential $\vec{A}$ are

$$H_{\rm em} = -\frac{\hbar\gamma_1 e k_z}{2m_0 C}\begin{pmatrix} 2(1-\mu)A_z & 0 & 3\mu A_x \\ 0 & 2(1-\mu)A_z & 3\mu A_y \\ 3\mu A_x & 3\mu A_y & 2(1+2\mu)A_z \end{pmatrix}. \tag{A18}$$

The results for the interband matrix elements are

$$\begin{aligned}
&\langle \mathrm{hh}\uparrow | H_{\rm em} | \mathrm{lh}, \mathrm{so}\uparrow\rangle = 0, \\
&\langle \mathrm{hh}\uparrow | H_{\rm em} | \mathrm{lh}, \mathrm{so}\downarrow\rangle = -\frac{\hbar\gamma_1 e k_z 3\mu x_\mp (A_x - iA_y)}{2m_0 c\sqrt{2}}, \\
&\langle \mathrm{lh}\uparrow | H_{\rm em} | \mathrm{so}\uparrow\rangle = -\frac{8\hbar\gamma_1 e\mu k_z A_z x_- x_+}{2m_c c}, \\
&\langle \mathrm{lh}\downarrow | H_{\rm em} | \mathrm{so}\uparrow\rangle = -\frac{\hbar\gamma_1 e 3\mu k_z (A_x - iA_y)}{2m_0 c} \\
&\qquad\qquad \times (y_+ x_- - y_- x_+).
\end{aligned} \tag{A19}$$

We note that because of the dependence of $x_\pm$ and $y_\pm$ on k the interband transitions have a more complex dependence on k than obtained in the limit of infinite spin-orbit splitting. For example, the transition rate for hh to so transitions increases by a factor of 3 between small and large k, while the rate for lh to so transitions decreases by a factor 81/209 between small and large k.

The cross section is now obtained from (A19) by using Fermi's rule for the transition rate for photons. The rate for band 1 to band 2 is

$$\frac{1}{\tau_{\rm ph}} = \frac{2\pi}{\hbar} V 2 \int \frac{d^3k}{(2\pi)^3} f_1^k (1 - f_2^k) |\langle 1 | H_{\rm em} | 2\rangle|^2 \times \delta(\hbar\omega + \hbar\omega_k^1 - \hbar\omega_k^2). \tag{A20}$$

Take the matrix elements of the vector potential between states of $N_{\rm ph}$ and $N_{\rm ph} - 1$ photons, using

$$\vec{A} = \frac{1}{L^{3/2}} \sum_{k\lambda} \vec{\epsilon}_{k\lambda} \left(\frac{2\pi\hbar_c}{k}\right)^{1/2} \{\hat{C}_{k\lambda} \exp[i(\vec{k}\cdot\vec{r} - kct)] + \hat{C}_{k\lambda}^\dagger \exp[-i(\vec{k}\cdot\vec{r} - kct)]\}. \tag{A21}$$

Here $\hat{C}_{k\lambda}$ and $\hat{C}_{k\lambda}^\dagger$ are creation and annihilation operators, respectively, and $k = \omega/c\sqrt{\epsilon_R}$. Then use

$$\sigma n_h N_{\rm ph} c = 1/\tau_{\rm ph}, \tag{A22}$$

and take the angular average $\langle A_x^2 \rangle = \frac{1}{3}A^2$. This produces the same result as (A17). This may be shown by using the relations

$$\lim_{q\to 0} \frac{1}{2} \int_{-1}^{1} d\cos\theta_{\vec{k},\vec{q}} \sin^2\theta_{\vec{k},\vec{k}+\vec{q}} = \frac{2q^2}{3k^2}. \tag{A23}$$

Thus, the cross section for heavy-hole to spin-orbit transitions in the spherical model is

$$\sigma_h^{\mathrm{hh}\to\mathrm{so}} = \frac{\pi^2\mu^2\hbar^2\gamma_1^2 e^2}{n_h c m_0^2 \omega(\epsilon_R)^{1/2}} \int \frac{d^3k}{(2\pi)^3} f_{\rm hh}^k k^2 6 |x_+^k|^2 \times \delta(\hbar\omega + \epsilon_k^{\rm hh} - \epsilon_k^{\rm so}). \tag{A24}$$

The cross section for light-hole to spin-orbit transitions in the spherical model is

$$\sigma_h^{\mathrm{lh}\to\mathrm{so}} = \frac{\pi^2\mu^2\hbar^2\gamma_1^2 e^2}{n_h c m_0^2 \omega(\epsilon_R)^{1/2}} \int \frac{d^3k}{(2\pi)^3} f_k^{\rm lh} k^2 \left(\frac{128}{3}(x_- x_+)^2 + 12(y_+ x_- - y_- x_+)^2\right) \delta(\hbar\omega + \epsilon_k^{\rm lh} - \epsilon_k^{\rm so}). \tag{A25}$$

The imaginary part of the dielectric function for nonzero q enters into the expressions for line shapes obtained in the main text. The important new feature of diamond and zinc-blende semiconductors compared to single component plasmas is that the heavy-hole to light-hole transitions damp the plasmon. In Fig. 13 we exhibit regions of the ω, q plane where contributions to the imaginary part of dielectric function are nonzero in the spherical approximation. The contribution of electron-electron transitions are shown with left slanted hatching, the heavy-hole to heavy hole are shown with right slanted hatching, and the heavy-hole to light-hole contribution is shown with vertical hatching. The heavy solid line shows the plasmon dispersion in the absence of heavy-hole to light-hole transitions. A popular approximation is to replace this complex excitation spectrum for the electron-hole plasma by a single-plasmon pole.[23] In the main text, it is argued that this approximation is the reason that nondivergent answers were obtained in a previous theory of

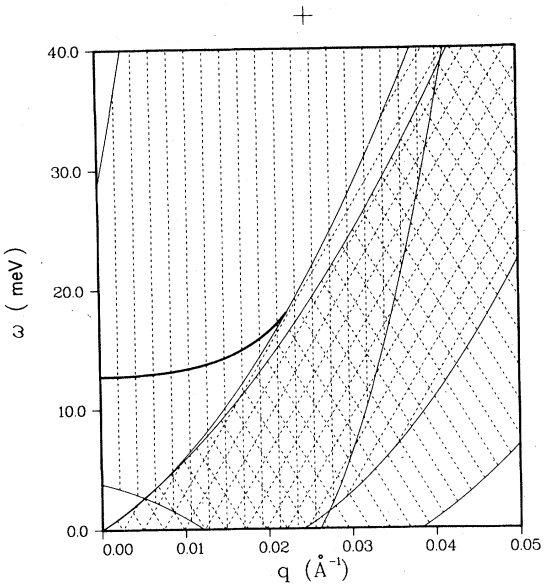

FIG. 13. Excitation spectrum of the electron-hole droplets in Ge in the spherical model for the valence-band structure. The hatched regions show where contributions to the imaginary part of the dielectric function are nonzero. The right-slanted hatching is for electron to electron transitions, the left-slanted is for heavy-hole to heavy-hole transitions, and the vertical hatching is for heavy-hole to light-hole transitions. The thick solid line denotes the plasmon position in the absence of damping by heavy-hole to light-hole transitions.

line shapes for direct-gap gain spectra.[7] It is clear from Fig. 13 that this is a poor approximation to the true excitation spectrum of an electron-hole plasma in semiconductors with degenerate valence bands.

APPENDIX B: DETAILS OF THE MULTIPLE-SCATTERING WAVE FUNCTION

In order to carry out manipulations with the ansatz multiple-scattering wave function, Eq. (8), it is useful to convert to box normalization. Thus, in a volume V one has

$$(2\pi)^3\delta(k-k') \to (1/V)\delta_{kk'} \tag{B1}$$

and

$$\int \frac{d^3k}{(2\pi)^3} \to \frac{1}{V}\sum_k . \tag{B2}$$

Then, using the definition of $\Sigma(k)$, the Eq. (8) may be written

$$\langle k|\psi^M_{k'}\rangle = \frac{1}{V}\sum_{j=1}^{N}\frac{\exp[i(\vec{k}-\vec{k}^1)\cdot\vec{r}_j]\langle\vec{k}|V|\psi^0_{\vec{k}'}\rangle}{\epsilon_{\vec{k}}+\Sigma(k)-\epsilon_{\vec{k}'}} \times(\delta_{\vec{k}\vec{k}'}-1). \tag{B3}$$

Thus, it is clear that (B3) satisfies the extinction theorem because the forward scattering component $\vec{k}=\vec{k}'$ is zero. Here N is the number of impurities in the volume V.

To derive Eq. (9), Eq. (B3) must be squared and impurity averaged:

$$|\langle k|\psi^M_{k'}\rangle|^2 = \left|\frac{1}{V}\frac{(\delta_{\vec{k}\vec{k}'}-1)\langle\vec{k}|V|\psi_{\vec{k}'}\rangle}{\epsilon_{\vec{k}}+\Sigma(k)-\epsilon_{\vec{k}'}}\right|^2 \times\left(\sum_{j=1}^{N}\sum_{l\neq j}\exp i(\vec{k}-\vec{k}')(\vec{r}_j-\vec{r}_l)+N\right). \tag{B4}$$

The impurity average of the first term in the brackets in (B4) is nonzero only for $\vec{k}=\vec{k}'$, and is therefore killed by the $\delta_{\vec{k}\vec{k}'}-1$ term. Thus, Eq. (9) follows.

[1]For a review, see T. M. Rice, J. C. Hensel, T. G. Phillips, G. A. Thomas, *Solid State Physics*, edited by H. Ehrenreich, F. Seitz, and D. Turnbull (Academic, New York, 1977), Vol. 32.

[2]Ya. E. Pokrovsky, Phys. Status Solidi 11, 3851 (1972); G. A. Thomas, T. G. Phillips, T. M. Rice, and J. C. Hensel, Phys. Rev. Lett. 31, 386 (1973); R. B. Hammond, T. C. McGill, and J. W. Mayer, Phys. Rev. B 13, 3566 (1976).

[3]G. Gobel, Appl. Phys. Lett. 24, 492 (1974); T. S. Moss, G. T. Burell and B. Ellis, *Semiconductor Optoelectronics* (Wiley, New York, 1973), p. 231ff; R. F. Leheny and J. Shah, Phys. Rev. Lett. 38, 511 (1977); R. Luzzi and L. C. M. Miranda, Phys. Rep. 43, 423–453 (1978).

[4]V. N. Murzin, V. A. Zayats, and V. L. Kononenko, Fiz. Tverd. Tela 17, 2684 (1976) [Sov. Phys. Solid State 17, 1783 (1976)]; J. H. Rose, H. B. Shore, and T. M. Rice, Phys. Rev. B 17, 752 (1978); H. G. Zarate and T. Timusk (unpublished).

[5]Ya. E. Pokrovsky and K. I. Svistunova, Fiz. Tverd. Tela 13, 2788 (1971) [Sov. Phys. Solid State 13, 2334 (1972)]. These measurements have been repeated by M. Glicksman, S. Mittleman, and J. R. Meyer (unpublished).

[6]P. T. Landsberg, Phys. Status Solidi 15, 623 (1966).

[7]W. F. Brinkman and P. A. Lee, Phys. Rev. Lett. 31, 257 (1973).

[8]M. Combescot and P. Nozières, J. Phys. C 5, 2369 (1972); W. F. Brinkman and T. M. Rice, Phys. Rev. B 7, 1508 (1973); P. Vashishta, P. Bhattachaya, and K. S. Singwi, Phys. Rev. Lett. 30, 1248 (1973); G. Beni and T. M. Rice, Phys. Rev. B 18, 768 (1978).

[9]R. N. Silver and C. H. Aldrich, Phys. Rev. Lett. 41, 1249 (1978).

[10]R. N. Silver and C. H. Aldrich, *Proceedings of the XIVth International Conference on the Physics of Semiconductors, Edinburgh*, 1978, edited by B. L. H.

Wilson (The Institute of Physics, London, 1978), p. 183.
[11]R. N. Silver (unpublished).
[12]J. M. Worlock, T. C. Damen, K. I. Shaklee, and J. P. Gordon, Phys. Rev. Lett. 33, 771 (1974).
[13]R. Luzzi and L. C. M. Miranda, Phys. Rep. 43, 423–453 (1978).
[14]R. W. Martin and H. L. Stormer, Solid State Commun. 22, 523–526 (1977).
[15]D. L. Smith, M. Chen, and T. C. McGill, Phys. Rev. B 14, 3504 (1976).
[16]See M. Lax, Rev. Mod. Phys. 23, 287 (1951) for a general discussion.
[17]T. M. Rice, Nuovo Cimento 23 B, 226 (1974); M. Rösler and R. Zimmerman, Phys. Status Solidi B 67, 525 (1975).
[18]A. Baldereschi and N. O. Lipari, Phys. Rev. B 8, 2697 (1973).
[19]See, for example, the discussion by W. Jones and N. H. March, in *Theoretical Solid State Physics* (Wiley-Interscience, New York, 1973), p. 190ff.
[20]M. Combescot and P. Nozières, Solid State Commun. 10, 301 (1972).
[21]J. H. Rose and H. B. Shore, Phys. Rev. B 17, 1884 (1978).
[22]E. O. Kane, J. Phys. Chem. Solids 1, 82 (1956).
[23]A. W. Overhauser, Phys. Rev. B 3, 1888 (1971); G. Mahler and J. L. Birman, *ibid.* 16, 1552 (1977).
[24]R. N. Silver and R. B. Hammond (unpublished).
[25]R. N. Silver (unpublished).